Journal of Nepal Geological Society, 2002, Vol. 26, pp. 1–6

Quantifying displacement on the South Tibetan Detachment normal fault, Everest massif, and the timing of crustal thickening and uplift in the Himalaya and South Tibet

***M. P. Searle[1], R. L. Simpson[1], R. D. Law[2], D. J. Waters[1], and R. R. Parrish[3]**
[1]*Department of Earth Sciences, Oxford University, Parks Road, Oxford OX1 3PR, UK*
*(*Corresponding author, e-mail: Mike.Searle@earth.ox.ac.uk)*
[2]*Geological Sciences, Virginia Tech., Blacksburg, Virginia 24061, USA*
[3]*Department of Geology, Leicester University, Leicester LE1 7RH, and NERC Isotope Geosciences Laboratory, Keyworth, Nottingham, NG12 5GG, UK*

ABSTRACT

Lithospheric convergence of India and Asia since collision has resulted in horizontal shortening, crustal thickening and regional metamorphism in the Himalaya and beneath southern Tibet. The boundary between the High Himalaya and the Tibetan plateau is a large scale, north-dipping, low-angle normal fault termed the South Tibetan Detachment (STD) which was active contemporaneously with the Main Central Thrust (MCT) bounding the southern margin of the High Himalaya. Previous studies have estimated minimum northward displacement along the STD of 35 km along the Everest profile. Here, we demonstrate approximately 200 km of southward displacement of footwall sillimanite + cordierite gneisses (minimum 90-108 km), formed at 600-630°C and pressures of 4.0-4.9 kbar (14-18 km depth), beneath the STD which acted as a passive roof fault during southward flow of the hot, viscous, ductile middle crust. U-Th-Pb dating of gneisses, sheared and cross-cutting leucogranites indicates that ductile shearing was active at 17-16 Ma, and later brittle motion at <16 Ma cuts all rocks in the footwall. High temperatures (>620°C) were maintained for ~14 Ma along the top of the High Himalayan slab from 32-18 Ma, implying active crustal thickening and high topography in south Tibet during this time. The ending of metamorphism and melting in the Himalaya and ductile shearing along the STD coincides with the initiation of strike-slip faulting in SW Tibet and E-W extension in south Tibet.

INTRODUCTION

Deep seismic reflection profiling across southern Tibet from project INDEPTH (Zhao et al. 1993; Nelson et al. 1996), combined with broadband earthquake and magnetotelluric data (Wei et al. 2001) have suggested that a high-conductivity layer at 15-20 km depth reflects partial melts and/or aqueous fluids in the middle crust of southern Tibet (Nelson et al. 1996; Alsdorf and Nelson 1999). High geothermal activity and high heat flow (Francheteau et al. 1984) at shallow levels in the crust are most likely due to aqueous fluids. Satellite magnetic data reveal a low over Tibet indicating hot crust, and the deeper levels of the high-conductivity zone have been interpreted as *in situ* partial melting (Alsdorf and Nelson 1999). Several factors such as radiogenic heating and crustal thickening and shortening could have induced the high temperatures at these mid-crustal levels beneath southern Tibet. Seismological data show that relatively fast (cool) upper mantle extends from the Himalaya northwards to roughly the center of the Tibetan plateau (Owens and Zandt 1997). The crustal structure of southern Tibet, as determined from the INDEPTH profile, shows several reflectors which have been successfully matched to the major faults of the Himalaya to the south, notably the South Tibetan Detachment (STD) and the Main Himalayan Thrust (MHT; Hauck et al. 1998; Alsdorf et al. 1998). It has further been suggested that ages of crustal melt leucogranites in the footwall of the STD decrease to the north (Wu et al. 1998) and that the Greater Himalayan crystalline rocks bounded by the STD above and the Main Central Thrust (MCT) below have been effectively extruded southwards from beneath the middle crust of south Tibet (Grujic et al. 1996, 2002; Searle 1999).

Here, we use new structural, metamorphic and thermobarometric data from the Everest region of Nepal and south Tibet (Fig. 1) to determine the P-T conditions (Fig. 2) and depths of formation of the footwall rocks beneath the STD. We use these data to quantify the amount of extension along the fault (Fig. 1c), and hence the minimum amounts of southward extrusion of these mid-crustal rocks. We also use U-Th-Pb dating of metamorphic rocks and leucogranites in the footwall of the STD (Hodges et al. 1998; Murphy and Harrison 1999; Simpson et al. 2000) to provide time constraints of metamorphism, melting, cooling and ductile-brittle shearing along the STD.

THE EVEREST MASSIF

In the Everest region the STD consists of two normal faults, the upper Qomolangma Detachment (QD) which places Ordovician sedimentary rocks above greenschist facies carbonates and shales (Burchfiel et al. 1992; Hodges et al. 1998; Searle 1999), and the lower Lhotse Detachment (LD)

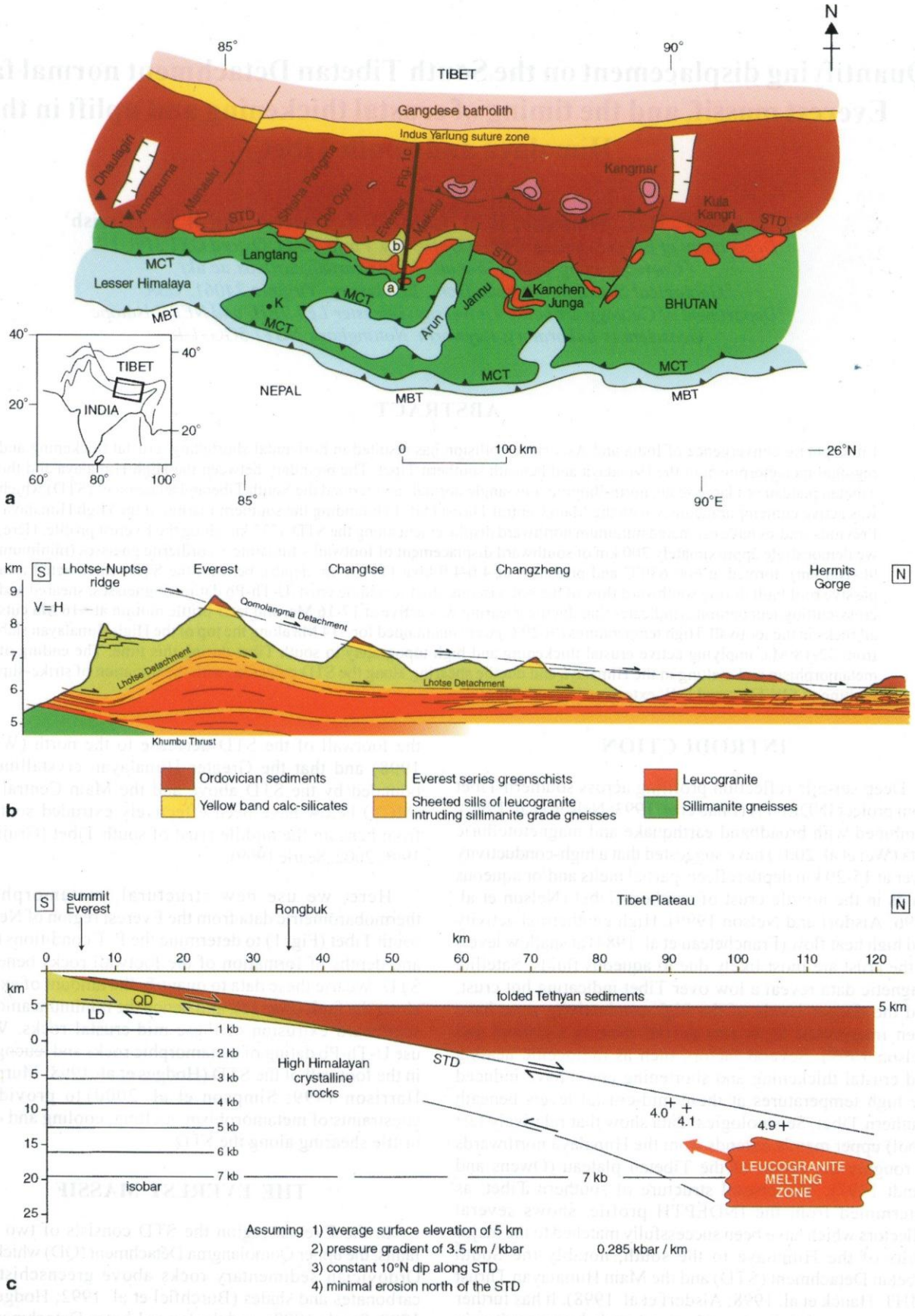

Fig. 1: Caption in the facing page.

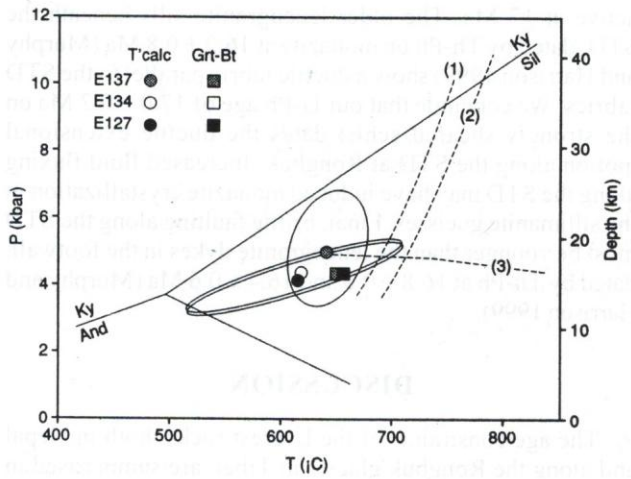

Fig. 2: Summary of thermobarometric results for the Kala Patthar rocks. Circles show results from THERMOCALC with corresponding error ellipses. Squares show results from Grt-Bt thermometry. Reactions: (1) Ms + Ab + Qtz = Kfs + As + Melt, (2) Ms + An + Qtz = Kfs + As + Melt. (3) Alm + Sil + Qtz + V = FeCrd.

which places the Everest series greenschists above high-grade sillimanite – cordierite gneisses with more than 50% leucogranite sills and sheets (Fig. 1; Searle 1999). The dip of the QD on the upper slopes of Everest is between 10-12°N shallowing to 4-5°N on the peak of Changtse and between 3°N and horizontal along the Rongbuk glacier and to the north (Fig. 1b). The QD merges with the LD near Rongbuk to form one large shear zone. Along the Nepal-Tibet border the STD dips consistently north and matches a prominent reflector in the INDEPTH profile to the east which dips at around 10°N (Zhao et al. 1993; Nelson et al. 1996; Hauck et al. 1998). The pattern of preferred quartz c-axis orientation in the gneisses beneath the LD indicates that penetrative deformation was close to plane strain. The sense of asymmetry is consistent with top down-to-north shear sense. Sillimanite grains have been drawn into the extensional shear bands but still appear pristine, suggesting that penetrative deformation occurred at close to peak metamorphic temperatures. Plastically deformed feldspars suggest temperatures above 450–500°C. There is little or no evidence for a later, lower temperature greenschist facies overprint. These "quenched" fabrics support models for rapid exhumation along the footwall of the STD. The dominant microstructural shear sense indicators (extensional shear bands, mica fish, porphyroclast tails etc) indicate top-down-to-NNE sense of shear. However, both top-to-north and top-to south shear bands have developed contemporaneously (Law et al. 2001). Both ductile simple shearing and pure shear coaxial deformation are distributed through the Greater Himalayan sequence metamorphic rocks.

THERMOBAROMETRY

Three samples collected from Kala Patar, a small peak near Everest Base camp on the Nepalese side of the mountain, contain appropriate assemblages for thermobarometric estimates using an internally consistent thermodynamic dataset (Holland and Powell 1998) with the THERMOCALC computer programme (version 2.75; original documentation in Powell and Holland 1988). Samples E127, E134 (both Crd + Grt + Sil + Bt + Pl + Qtz) and E137 (Grt + Sil + Bt + Pl + Kfs + Qtz) yielded final equilibrium conditions of 623 ± 79°C, 4.0 ± 0.8 kbar, 626 ± 79°C, 4.1 ± 0.8 kbar and 651 ± 41°C, 4.9 ± 1.4 kbar, respectively. Independent garnet-biotite and garnet-cordierite thermometers yield similar temperatures. Samples collected from immediately beneath the STD at Rongbuk monastery are devoid of garnet and therefore have unsuitable assemblages from which to obtain pressure estimates. Two feldspar thermometry fails to retrieve peak temperatures from these rocks due to late-stage unmixing reducing the albite content of orthoclase. We therefore use the samples from Kala Patar for our structural restoration (Fig. 1c) as we believe they record true peak conditions, which suggest temperatures of at least 620°C at depths of around 14-18 km.

Assuming a constant dip of 10° of the STD north of Rongbuk and a pressure gradient of 3.5 km/kbar, we obtain horizontal displacements of footwall High Himalayan rocks of 90-108 km (Fig. 1c). This is a conservative estimate for the amount of displacement; if we use a more realistic 5° dip of the STD, as mapped along the Rongbuk glacier, we obtain horizontal displacements of footwall High Himalayan rocks of 180-216 km southwards. The geometry of the restored Everest - Rongbuk profile explains the 40 km wide isothermal

Fig. 1a: Geological sketch map of the Nepal-South Tibet Himalaya. The line of section in Fig. 1c is shown from Everest northwards. a is the location of Kala Patar and the samples used for thermobarometry, b is the location of the Rongbuk glacier. K- Kathmandu.

b: Cross-section across the Everest massif and southern Tibetan Plateau along the Rongbuk glacier profile.

c: Restored section across the Everest-south Tibetan plateau region. The upper Qomolangma Detachment (QD) and lower Lhotse Detachment (LD) are both part of the South Tibetan Detachment (STD) series of low-angle normal faults. Crosses mark the restored positions and depths of three samples from Kala Patar, 2 km SW of Everest, which record pressures of 4.0, 4.1 and 4.9 kbar. Using an average 10° dip of the STD the relative southward displacement of the sillimanite grade rocks along the footwall is 90–108 km. The true dip of the STD as measured on the north face of Everest and along the Rongbuk glacier is between 3-5° N; at this angle of dip the relative displacement along the STD would be 180-216 km. The approximate depth and original position of the Everest leucogranites prior to emplacement along the footwall of the STD is also shown.

exhumation of the high grade sillimanite gneisses in the Nepal Himalaya south of Everest, bounded by the MCT below and the STD above, and this is compatible with the origin of the Greater Himalayan rocks from mid-crustal levels (4-5 kbar; 15-18 km depth) beneath the southern Tibetan plateau.

U-Pb GEOCHRONOLOGY

Sample E282, a strongly foliated Qtz + Pl + Bt + Mc + Sil schist was collected from immediately below the STD at Rongbuk (locality b on Fig. 1a) for U-Pb dating (Fig. 3). Three multi-grain monazite fractions, comprising crystals about 60 microns in diameter were hand-picked for analysis. Two fractions, M1 and M3, plot concordantly at 16.95 ± 0.15 Ma and have low Th/U ratios. Fraction M2 plots below concordia at 17.5-17.8 Ma. It could be that ages of M1 and M3 result from Pb-loss from 22 Ma grains, the age of cordierite-forming metamorphism recorded by sillimanite gneisses from Kala Patar (Simpson et al. 2000). Pb diffusion studies of monazite, however, suggest that grains of this size heated at 650°C would have to lose upwards of 40% of their Pb to plot at 17 Ma (Smith and Giletti 1997). The fact that both fractions are concordant strongly argues against Pb-loss of this magnitude, and we therefore discount this possibility. Taking into consideration discordant fraction M2, it is then possible that the concordant fractions at 17 Ma are mixtures of an older (circa 500 Ma) detrital component and a younger episode of growth that occurred more recently than 17 Ma. The fact that the two multi-grain fractions M1 and M3 plot with overlap combined with the generally homogeneous chemical nature of these crystals (revealed by microprobe mapping) suggests, however, that the analysed crystals are not comprised of zones of growth at different ages. We therefore interpret the age of this sample as 17.0 ± 0.2 Ma.

It is no coincidence that the youngest monazite ages in the Greater Himalayan Crystallines are found closest to the STD. Both Th-Pb dating (Murphy and Harrison 1999) and $^{40}Ar/^{39}Ar$ dating (Hodges et al. 1998) of leucogranites in the footwall of the STD at Rongbuk suggest that the fault was active at 17 Ma. The older leucogranite sills beneath the STD, dated by Th-Pb on monazite at 16.2 ± 0.8 Ma (Murphy and Harrison 1999) show a ductile fabric parallel to the STD fabrics. We conclude that our U-Pb age of 17.0 ± 0.2 Ma on the strongly sheared schist dates the ductile extensional motion along the STD at Rongbuk. Increased fluid fluxing along the STD may have induced monazite crystallization in the sillimanite gneisses. Final, brittle faulting along the STD must be younger than the leucogranite dykes in the footwall, dated by Th-Pb at 16.8 ± 0.8 and 16.4 ± 0.6 Ma (Murphy and Harrison 1999).

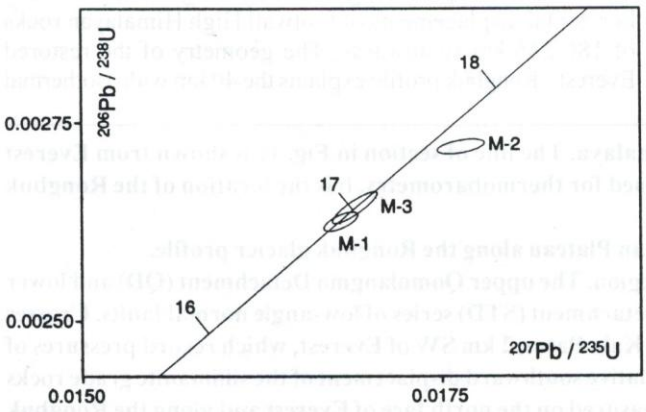

Fig. 3: U-Pb concordia diagram for sample E282 (see text for discussion).

DISCUSSION

The age constraints of the Everest rocks, both in Nepal and along the Rongbuk glacier in Tibet, are summarised in Fig. 4. These ages reveal that peak burial metamorphism occurred at 32.2±0.4 Ma (Simpson et al. 2000), and temperatures remained high (~600-700°C) for about 15 Ma until about 16 Ma when ductile shear along the STD ceased, and brittle faulting truncated all the rocks in the footwall. Such temperatures could have remained high for so long, only if active crustal shortening and thickening was occurring throughout that time. Thick crust and high temperature imply that the surface elevation must also have been high. It is impossible to precisely constrain the amount of palaeo-elevation of southern Tibet during the period 32-16 Ma; all we can say is that our data do not support models for the sudden and rapid increase in elevation of the plateau at 7-8 Ma (Molnar et al. 1993) or younger Pliocene-Quaternary ages based on nearest modern relatives of fossil plants (Xu 1981).

We suggest, from the structural and geochronological data from the Everest region (Fig. 4), that crustal melting of

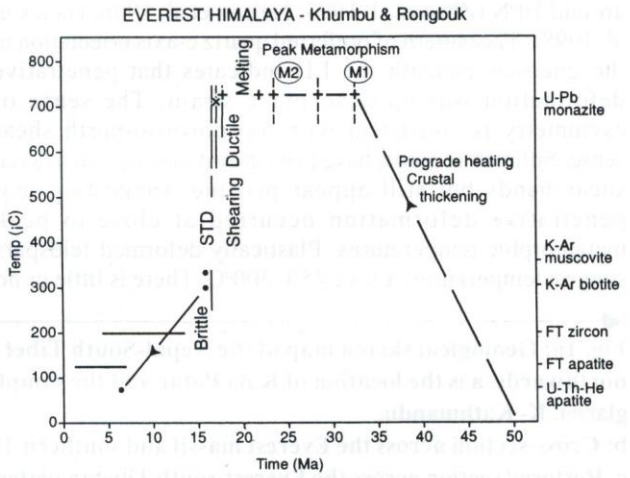

Fig. 4: Summary chart of the metamorphic and granitic rocks in the Everest region of Nepal–South Tibet (see text for sources of data). Closure temperatures for various minerals are shown on the right with the exception of monazite, whose dates are interpreted as growth ages according to individual magmatic or metamorphic (P-T) conditions.

the High Himalayan granites (21-16 Ma; Murphy and Harrison 1999; Simpson et al. 2000) triggered sudden and rapid extrusion, by viscous flow, of the partially melted middle crust of the High Himalaya along the footwall of the STD. The hanging wall sedimentary rocks above the STD, which were shortened by folding and thrusting during the early part of the India-Asia collision (late Eocene – Oligocene) were not buried to depth or metamorphosed and were subjected to minimal erosion. Rapid extrusion of the Greater Himalayan metamorphic rocks resulted in rapid cooling during exhumation when temperatures decreased from ~700°C–300°C in <0.5 Ma This sudden, rapid cooling is common to all well-dated High Himalayan granites (e.g., Searle et al. 1997, 1999) and implies that the entire High Himalayan chain probably reached its maximum elevation during the period 21-16 Ma when erosion levels along the Himalaya, in contrast to the Tibetan plateau, were extremely high. The timing of this coincides roughly with initiation of some of the major strike-slip faults bounding the thickened crust of Tibet (e.g., ~17 Ma for the Karakoram fault; Searle et al. 1998), the timing of initiation of E-W extension with the intrusion of potassic and ultra-potassic shoshonitic dykes (~18-13 Ma; Miller et al. 1999; Williams et al. 2001) and the later development of the major N-S graben systems such as the Thakhola graben at 13-10 Ma (Coleman and Hodges 1995: Garzione et al. 2000).

Our results support the model from the INDEPTH seismic experiments which suggest the presence of a regional mid-crustal layer of partially molten rock where granite minimum melt temperatures (>600-650°C) were at 15-18 km depth beneath Tibet (Nelson et al. 1996; Alsdorf and Nelson 1999). Our thermobarometric data show that peak metamorphic pressures relate to similar depths (14-18 km). Our data also support models of fluid flow of a ductile middle or lower crust (Royden et al. 1997; Clark and Royden 2000), and can place a lower bound on the amount of southward extrusion along the footwall of the STD of 150–200 km. The amounts of crustal shortening in the Indian plate Tethyan zone upper crust between the STD and the Indus Suture Zone (Searle et al. 1988) roughly balances the amounts of underthrusting of Indian lower crust northwards as far as the Bangong suture (150–300 km; Owens and Zandt 1997). Our structural, metamorphic and thermobarometric data from the Everest massif prove that the crust beneath southern Tibet is rheologically layered with regional scale, sub-horizontal detachments or shear zones separating crust which was deformed by different amounts and at different times. The middle crust beneath southern Tibet and the Himalaya is a weak, ductile deforming zone of high heat and low friction separating a brittle deforming upper crust above from a strong (?granulite facies) lower crust with a rheologically strong upper mantle.

ACKNOWLEDGEMENTS

This work was funded by the Royal Society and NERC grants. We thank Rene Shrama, Shiva Dhakal, Tsering and Tasi Sherpa for logistical help.

REFERENCES

Alsdorf, D., Brown, L., Nelson, K. D., Makovsky, Y., Klemperer, S., and Zhao, W., 1998, Crustal deformation of the Lhasa terrane, Tibet plateau from Project INDEPTH deep seismic reflection profiles. Tectonics, v. 17, pp. 501–519.

Alsdorf, D. and Nelson, K. D. 1999, Tibetan satellite magnetic low: Evidence for widespread melt in the Tibetan crust? Geology, v. 27, pp. 943–953.

Burchfiel, B. C., Zhiliang, C., Hodges, K. V., Yuping, L., Royden, L. H., Changrong, D., and Jiene, X., 1992, The South Tibetan detachment system, Himalayan orogen: Extension contemporaneous with and parallel to shortening in a collisional mountain belt. Geol. Soc. America Special Paper, v. 269, 41 p.

Clark, M. K. and Royden, L. H., 2000, Topographic ooze: Building the eastern margin of Tibet by lower crustal flow. Geology, v. 28, pp. 703–706.

Coleman, M. and Hodges, K., 1995, Evidence for Tibetan plateau uplift before 14 Myr from a new minimum age for east-west extension. Nature, v. 374, pp. 49–52.

Francheteau, J., Jaupart, C., Jie, S. X., et al., 1984, High heat flow in southern Tibet. Nature, v. 307, pp. 32-34.

Garzione, C. N., Dettman, D. L., Quade, J., DeCelles, P. G., and Butler, R. F., 2000, High times on the Tibetan plateau: Paleoelevation of the Thakkola graben, Nepal. Geology, v. 28, pp. 339–342.

Grujic, D., Casey, M., Davidson, C., Hollister, L. S., Kundig, R., Pavlis,T., and Schmid, S., 1996, Ductile extrusion of the High Himlalayan crystalline in Bhutan: evidence from quartz microfabrics.Tectonophysics, v. 260, pp. 21-43.

Grujic, D., Hollister, L., and Parrish, R. R., 2002, Himalayan metamorphic sequence as an orogenic channel: insight from Bhutan. Earth & Planetary science letters, v. 198, pp. 177-191.

Hauck, M. L., Nelson, K. D., Brown, L. D., Zhao, W., and Ross, A. R., 1998, Crustal structure of the Himalayan orogen at ~90°east longitude from Project INDEPTH deep seismic reflection profiles. Tectonics, v. 17, pp. 481–500.

Hodges, K., Bowring, S., Davidek, K., Hawkins, D., and Krol, M., 1998, Evidence for rapid displacement on Himalayan normal faults and the importance of tectonic denudation in the evolution of mountain ranges. Geology, v. 26, pp. 483–486.

Holland, T. J. B. and Powell, R., 1998, An internally consistent thermodynamic dataset for phases of petological interest. Jour. Metam. Geol., v. 16, pp. 309–344.

Law, R. D., Searle, M. P., and Simpson, R. L., 2001, Microstructural and quartz petrofabric evidence for strain paths and deformation temperatures, South Tibetan detachment system, Everest massif, South Tibet. Journal Asian Earth Sciences, v. 19 (3A), 38 p.

Miller, C., Schuster, R., Klotzli, U., Mair, V., Frank, W., and Purtscheller, F., 1999, Post-Collisional Potassic and Ultrapotassic magmatism in SW Tibet: Geochemical and Sr-Nd-Pb-O isotopic constraints for mantle source characteristics and petrogenesis. J. Petrology, v. 40, pp. 1399–1424.

Molnar, P., England, P., and Martinod, J., 1993, Mantle dynamics, uplift of the Tibetan plateau, and the Indian monsoon. Reviews of Geophysics, v. 31, pp. 357–396.

Murphy, M. A. and Harrison, T. M., 1999, Relationship between leucogranites and the Qomolangma detachment in the Rongbuk Valley, south Tibet. Geology, v. 27, pp. 831–834.

Nelson, K. D., Zhao, W., Brown, L., et al. 1996, Partially molten middle crust beneath southern Tibet: Synthesis of Project INDEPTH results. Science, v. 274, pp. 1684-1688.

Owens, T. J. and Zandt, G., 1997, Implications of crustal property variations for models of Tibetan plateau evolution. Nature, v. 387, pp. 37–42.

Powell, R. and Holland, T. J. B., 1988, An internally consistent dataset with uncertainties and correlations: 3. Applications to geobaromentry, worked samples and a computer programme. Jour. Metam. Geol., v. 6, pp. 173–204.

Royden, L. H., Burchfiel, B. C., King, R. W., Wang, E., Chen, Z., Shen, F., and Liu, Y., 1997, Surface deformation and lower crustal flow in eastern Tibet. Science, v. 276, pp. 788–790.

Searle, M. P., 1999, Extensional and compressional faults in the Everest – Lhotse massif, Khumbu Himalaya, Nepal. Jour. Geol. Soc. London, v. 156, pp. 227–240.

Searle, M. P., Cooper, D. J. W., and Rex, A. J., 1988, Collision tectonics of the Ladakh – Zanskar Himalaya. Royal Society, London, Philosophical transactions, v. A326, pp. 117–150.

Searle, M. P., Parrish, R. R., Hodges, K. V., Hurford, A. J., Ayres, M. W., and Whitehouse, M. J., 1997, Shisha Pangma leucogranite, South Tibetan Himalaya; Field relations, geochemistry, age, origin and emplacement. Jour. Geol., v. 105, pp. 295–317.

Searle, M. P., Weinberg, R. F., and Dunlap, W. J., 1998, Transpressional tectonics along the Karakoram fault zone, northern Ladakh: constraints on Tibetan extrusion. In: Holdsworth, R. E., Strachan, R. A., and Dewey, J. F. (eds.) Continental Transpressional and Transtensional Tectonics. Geol. Soc. London, Special Publ., v. 135, p. 307–326.

Searle, M. P., Noble, S. R., Hurford, A. J., and Rex, D. C., 1999, Age of crustal melting, emplacement and exhumation history of the Shivling leucogranite, Garhwal Himalaya. Geological Magazine, v. 136, p. 513-525.

Simpson, R. L., Parrish, R. R., Searle, M. P., and Waters, D. J., 2000, Two episodes of monazite crystallization during metamorphism and crustal melting in the Everest region of the Nepalese Himalaya. Geology, v. 28, p. 403-406.

Smith, H. A. and Giletti, B. J., 1997, Lead diffusion in monazite. Geoch. Cosmoch. Act, v. 61, p. 1047-1055.

Wei, W., Unsworth, M., Jones, A., Booker, J., Tan, H., Nelson, K. D., Chen L., Li, S., Solon, K., Bedrosian, P., Jin, S., Deng, M., Ledo, J., Kay, D., and Roberts, B., 2001, Detection of widespread Fluids in the Tibetan crust by magnetotelluric studies. Science, v. 292, pp. 716-718.

Williams, H. M., Turner, S., Kelley, S., and Harris, N., 2001, Age and composition of dikes in Southern Tibet: New constraints on the timing of east-west extension and its relationship to postcollisional volcanism. Geology, v. 29(4), pp. 339-342.

Wu, C., Nelson, K. D., Wortman, G., and Samson, S. D., 1998, Yadong cross structure and South Tibetan Detachment in the east central Himalaya (89°–90° E). Tectonics, v. 17, p. 28-45.

Xu, R., 1981, Vegetational changes in the past and uplift of the Qinghai-Xizang plateau. In: Geological and Ecological studies of the Qinghai-Xizang plateau, Beijing. Science Press, v. 1, pp. 139-144.

Zhao, W., Nelson, K. D., Brown, L., et al., 1993, Deep seismic reflection evidence for continental underthrusting beneath southern Tibet. Nature, v. 366, pp. 557-559.